TISSUE ENGINEERING: Part A
Volume 16, Number 4, 2010

DOI: 10.1089/ten.tea.2009.0226

Functional Assessment of Skeletal Muscle Regeneration Utilizing Homologous Extracellular Matrix as Scaffolding

Edward K. Merritt, M.S.,[1] David W. Hammers, M.S.,[1] Matthew Tierney, B.S.,[1]
Laura J. Suggs, Ph.D.,[2] Thomas J. Walters, Ph.D.,[3] and Roger P. Farrar, Ph.D.[1]

The loss of a portion of skeletal muscle poses a unique challenge for the normal regeneration of muscle tissue. A transection injury with tissue loss will not heal due to the gap between muscle segments. A damage model was developed by removing a portion of the lateral gastrocnemius (GAS) of Sprague-Dawley rats. Maximal isometric, tetanic tension (P_o) was measured after the removal of either a small defect (0.5×1.0 cm) or a large defect (1.0×1.0 cm) piece of the GAS. *In situ* P_o immediately after creation of the defect was $88.3\pm2.0\%$ of the nonoperated contralateral GAS force for small defect and $76.9\pm3.2\%$ of control for large defect. No functional recovery occurred in either group over the course of 28 days. To enhance recovery, a homologous, decellularized, muscle extracellular matrix (ECM) was implanted into the 1×1 cm defect of the lateral GAS of Lewis rats. After 42 days, growth of blood vessels and myofibers into the ECM was apparent, but no restoration of P_o occurred. These data demonstrate the ability of the ECM to support muscle and blood vessel regeneration, but full recovery of function does not occur after 42 days.

Introduction

Skeletal muscle injuries, including strains, contusions, and lacerations, are well documented.[1–3] Most of these injuries, if given sufficient time, will repair themselves with partial or total restoration of function.[2] The repair of the muscular tissue is largely the result of proliferation of resident satellite cells and other progenitor cells, which are capable of moving to the injured area and differentiating into muscle, connective, and vascular tissues.[4,5]

Severe skeletal muscle injuries, such as those involving the loss of a substantial portion of muscle, connective tissue, and blood vessels, however, are not capable of full regeneration on their own. These types of injuries are seen in military personnel wounded-in-action, car accident and gun shot victims, and patients having undergone surgeries where the debridement of muscle tissue was necessary.[6] In fact, injuries to the soft tissue of the extremities comprise the largest number of wounds received by U.S. military personnel in war-time activities,[7] and operations performed on the extremities after battlefield injuries make up the highest percentage of surgical procedures.[8] Even when the limb can be saved, the initial damage and loss of muscle and surrounding tissue will leave the soldier with a permanent physical handicap.[9] The current standard of care for these injuries is autologous tissue transfer (muscle flaps). Muscle flaps are used to improve esthetics and provide bony coverage. Although recent reports describe functional free muscle transplantation in the forearm[10] and elbow,[11] these procedures are associated with significant donor-site morbidity and are not yet applicable to large muscle defects.

Complete surgical repair of a skeletal muscle defect is dependent on the ability of an implant to bridge the gap between the transected muscle segments and allow transmission of force between the two ends, as it is necessary for the proper orientation of regenerating muscle fibers and subsequent return of function.[12] The tension developed in the regenerating muscle also stimulates local release of growth factors that enhance regeneration.[13] The implant should also serve as a scaffold and allow the incorporation of regenerating muscle, connective, nerve, and blood vessel tissues.

Several types of constructs suitable for skeletal muscle repair are commercially available. Materials such as Dacron, Silastic, Marlex, Vicryl, and others are often used to repair congenital muscular defects of the abdominal wall, but the success of these grafts varies due to issues with biocompatibility[14] and inability to allow for cell ingrowth.[15] The grafts are considered successful when they contain the bowels and look esthetically normal, but most do not allow for the full incorporation of the original tissue they replace. Natural materials for repair can be better for biocompatibility, host cell incorporation, and for reducing infection risks. These

Departments of [1]Kinesiology and [2]Biomedical Engineering, The University of Texas at Austin, Austin, Texas.
[3]Department of Regenerative Medicine, U.S. Army Institute of Surgical Research, Fort Sam Houston, Texas.

Report Documentation Page

Form Approved
OMB No. 0704-0188

1. REPORT DATE	2. REPORT TYPE	3. DATES COVERED
01 APR 2010	**N/A**	**-**

4. TITLE AND SUBTITLE	5a. CONTRACT NUMBER
Functional assessment of skeletal muscle regeneration utilizing homologous extracellular matrix as scaffolding	5b. GRANT NUMBER
	5c. PROGRAM ELEMENT NUMBER
6. AUTHOR(S)	5d. PROJECT NUMBER
Merritt E. K., Hammers D. W., Tierney M., Suggs L. J., Walters T. J., Farrar R. P.,	5e. TASK NUMBER
	5f. WORK UNIT NUMBER
7. PERFORMING ORGANIZATION NAME(S) AND ADDRESS(ES)	8. PERFORMING ORGANIZATION REPORT NUMBER
United States Army Institute of Surgical Research, JBSA Fort Sam Houston, TX 78234	
9. SPONSORING/MONITORING AGENCY NAME(S) AND ADDRESS(ES)	10. SPONSOR/MONITOR'S ACRONYM(S)
	11. SPONSOR/MONITOR'S REPORT NUMBER(S)

12. DISTRIBUTION/AVAILABILITY STATEMENT
Approved for public release, distribution unlimited

13. SUPPLEMENTARY NOTES

14. ABSTRACT

15. SUBJECT TERMS

16. SECURITY CLASSIFICATION OF:			17. LIMITATION OF ABSTRACT	18. NUMBER OF PAGES	19a. NAME OF RESPONSIBLE PERSON
a. REPORT	b. ABSTRACT	c. THIS PAGE			
unclassified	**unclassified**	**unclassified**	**UU**	**12**	

have been used successfully for repair of abdominal wall defects and may well be applied to load-bearing muscle grafts in the future.

In skeletal muscle the extracellular matrix (ECM) is an important structural component for the development of muscle fibers,[16] providing the proper mechanical and chemical environment for the proliferation and differentiation of myogenic progenitor cells[17–19] as well as releasing chemical signals to the surrounding environment that attract macrophages and progenitor cells that aid in the repair process.[20–22] Allografts and xenografts of ECM from the integument, urinary bladder and small intestine have been employed in research to repair tissues in the clinical setting (for review see Badylak[23]).

This study was designed to evaluate whether a homologous graft of ECM from skeletal muscle could be implanted into a large muscle defect, and could provide the tensile strength for muscular force transmission as well as the proper environment for growth and differentiation of regenerating muscle tissue. Although some researchers have studied ECM implantation into nonload-bearing, defected muscles such as those of the abdominal wall,[24–26] implantation and functional analysis of ECM into a skeletal muscle defect of an active, load-bearing muscle has not been attempted. Therefore, the purpose of this study was to develop a model to study the regeneration of a skeletal muscle defect involving replacement of lost tissue with a decellularized ECM that could be readily assessed functionally, morphologically, and histologically.

Materials and Methods

Animals

The study was done in two stages. The first stage consisted of establishing the muscle defect model in male Sprague-Dawley (S-D) rats. Initial work in isolating the ECM through decellularization, as well as development of the *in vivo* model of assessment of muscular function, was established in the S-D rat strain. To be consistent, the laceration model and defect model were established in this same strain. The second phase was conducted in Lewis rats, an inbred strain, bred for transplantation experiments.

Both male S-D rats from colonies provided by the University of Texas at Austin Animal Resource Center and male Lewis rats obtained from Charles River Laboratories (Wilmington, MA) 6–9 months of age were used in this study. Rats were housed individually and maintained on a 12-h light/dark cycle. Rats were allowed *ad libitum* access to food (Rodent Chow; Harlan-Teklad, Indianapolis, IN) and water. Rats were randomly assigned to experimental groups. All experimental procedures were approved and conducted in accordance with guidelines set by the University of Texas at Austin Institutional Animal Care and Use Committee.

Experimental groups

S-D rats were divided into one of four groups: sham operated (SHAM), laceration only (LAC), small defect (SDEF), and large defect (LDEF). Surgeries were performed under aseptic conditions, and the rats anesthetized with IP injections of sodium pentobarbital (65 mg/kg). Rats in the LAC group had a 2 cm incision made on the lateral side of the lower limb parallel to the tibia. The biceps femoris muscle was separated from the tibia to expose the lateral side of the lateral gastrocnemius (LGAS) muscle. The muscle was lacerated with a #9 scalpel blade distal to the neuromuscular junction in line with the tibial tuberosity. The incision was 1 cm in length through the lateral side of the LGAS and through the full thickness of the muscle. The two contiguous portions of the LGAS were not sutured together. To close the wound, the biceps femoris muscle was reattached to the tibia using simple, interrupted, polypropylene suture (Prolene 5-0; Ethicon, San Angelo, TX), and the incision in the skin was closed with silk suture (Ethicon 4-0). Rats in the LAC groups were placed back in their home cages and allowed to recover for 42 days.

Rats in the SDEF and LDEF groups underwent the same procedure as those rats in the LAC groups; however, instead of a laceration, a full-thickness defect was created with two #9 scalpel blades separated by 0.5 cm (SDEF) or 1.0 cm (LDEF). The result is two lacerations each 1 cm in length and 0.5 cm or 1.0 cm apart. The tissue between the lacerations was excised with fine surgical scissors, and the free section of muscle removed and weighed. The average mass of the removed muscle defect from the S-D rats was 152 ± 10 mg and 306 ± 10 mg for the SDEF and LDEF groups, respectively, and was statistically significant. The mass of the SDEF was approximately 5% of the mass of the whole GAS, and the mass of the LDEF was approximately 10% of the mass of the whole GAS. The wound was closed as in the LAC group. Rats in the SDEF groups were immediately subjected to functional analysis ($n = 6$) or recovered for 14 days ($n = 6$). Rats in the LDEF groups were immediately subjected to functional analysis ($n = 8$) or allowed to recover for 14 days ($n = 7$), or 28 days ($n = 6$).

The surgery for the SHAM group ($n = 6$) was identical to that of the defect groups except no incision or defect was created in the LGAS. An incision in the skin and the biceps femoris was made, and the LGAS exposed and separated from the soleus. The biceps femoris and skin incisions were sutured as in the other groups, and the animals were returned to their cages and allowed to recover for 14 days.

After development of the model in the S-D rats, further experiments were conducted using the exact same defect model in Lewis rats, because they are better suited for transplantation experiments. The previously described defect surgery was performed on 48 Lewis rats and 1×1 cm piece of the LGAS was removed. The average mass of the muscle defect removed from the Lewis rats was 238 ± 6 mg and 224 ± 6 mg for the DEF ONLY and DEF/REP groups, respectively. The difference was not statistically significant. The defect removed accounted for approximately 20% of the total mass of the LGAS. No repair surgery was performed on 24 rats (DEF ONLY), but the other 24 rats were subjected to a repair of the defect (DEF/REP) with a homologous ECM cut to the dimensions of the injury as described below. Six rats from each group were evaluated functionally and histologically at each of the following days of recovery: 7, 14, 28, and 42.

ECM isolation

GAS muscles were removed from a separate group of male Lewis rats and decellularized using a method similar to

Borschel *et al.*,[27] but with several modifications. Upon extraction the muscles were placed in deionized water at 4°C for 1 day to cause cell swelling and membrane rupture. The muscle was placed in chloroform and continuously agitated for 4 to 5 days depending on its size. The muscle was rinsed with water and submerged in 2% sodium dodecyl sulfate (SDS) and agitated continuously. The SDS solution was changed twice per week until the cellular components were washed out. The remaining ECM was rinsed in a large volume of deionized water (10:1 v/w) over several days with solution changes each day to rid the ECM of SDS. To completely insure removal of SDS, the ECMs were rinsed for 4 h in a 0.1 M Tris buffer solution of pH 9.0. The ECM was then submerged in phosphate-buffered saline with 1% penicillin/streptomycin (Sigma-Aldrich, St. Louis, MO), exposed to ultraviolet light for at least 12 h, and stored at 4°C until ready for implantation. To insure complete decellularization, samples of prepared ECM were stained with Masson's trichrome and run on SDS–polyacrylamide gel electrophoresis gels. Portions of whole muscle and ECM were homogenized in a HEPES-containing buffer solution (pH 7.6) at equal mass to volume ratios, and were centrifuged at 1200 *g*. The resulting supernatants were boiled in Lameli's buffer. The blank samples contained only homogenization buffer boiled in Lameli's buffer. Equal volumes of each sample were loaded into a polyacrylamide gel consisting of a 5% stacking gel and a 12.5% running gel. The gel was run at constant current for 1 h. The gel was then was stained in biosafe Coomassie blue solution (Bio-Rad, Hercules, CA) for 30 min. The image was taken using the Chemidoc XRS system (Bio-Rad). Additionally, a scanning electron microscope (Zeiss Supra BP, Thornwood, NJ, at UT-Austin ICMB Core Facility) was used to obtain images of the ECM (Fig. 1). A colorimetric assay described by Arand *et al.*[28] to measure the content of SDS was performed to insure complete removal of SDS from the ECM.

The ECM was implanted in the muscle with the defect using a modified Kessler stitch (5-0 Prolene; Ethicon) with simple interrupted sutures on each of the three borders to hold the cut ends together and serve as markers for later analysis. The modified Kessler stitch was used because it has been shown to be the most effective way to suture the transected muscle segments back together.[29]

Force measurements

After the designated recovery time, the GAS muscles were isolated and subjected to functional measurements. A skin incision was made down the midline of the posterior portion of the lower limb from the popliteal area to the calcaneus. The skin was reflected to expose the biceps femoris that inserts along the distal portion of the tibia in rats. The biceps

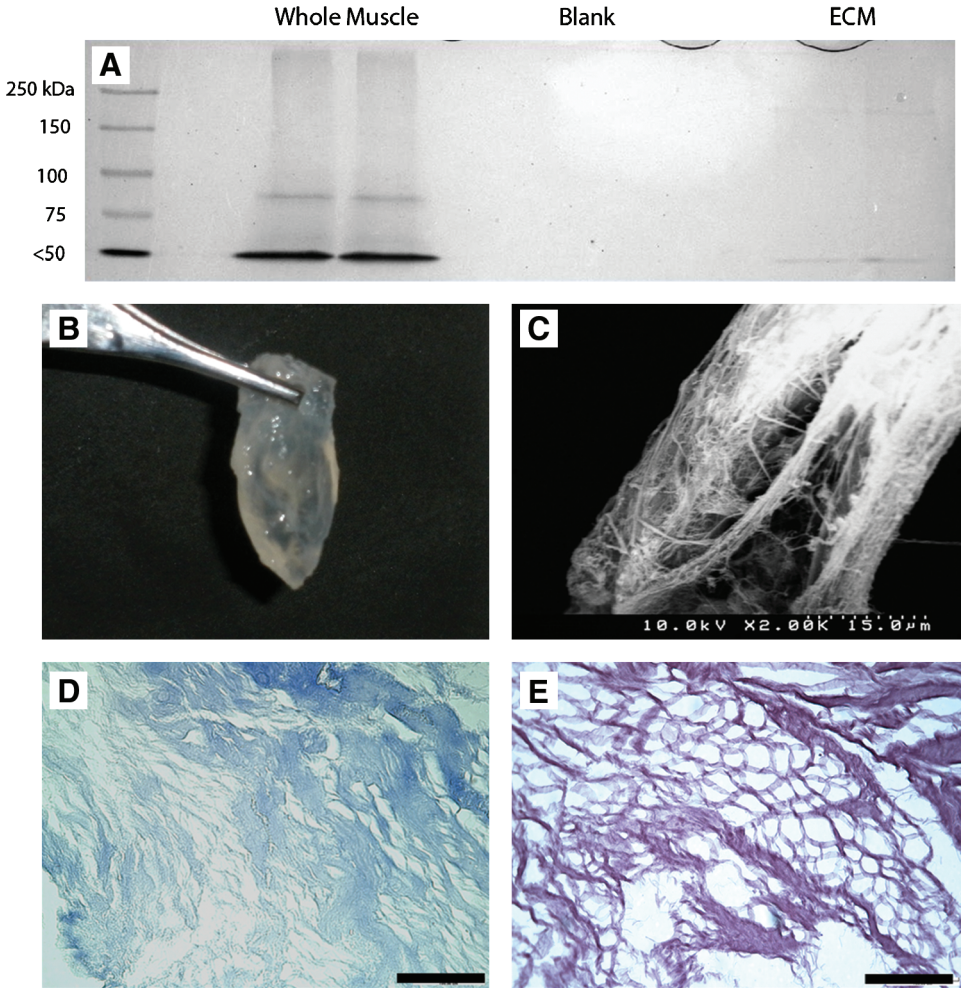

FIG. 1. (**A**) Coomassie staining of sodium dodecyl sulfate–polyacrylamide gel electrophoresis gel. (**B**) Visual appearance of decellularized ECM. (**C**) Scanning electron micrograph of ECM before implant. (**D, E**) Masson's trichrome stain and hematoxylin and eosin stain of ECM before implant (scale bars = 100 µm). ECM, extracellular matrix. Color images available online at www.liebertonline.com/ten.

femoris was cut and reflected to expose the medial and LGAS. With care to minimize bleeding and damage to surrounding tissues, the LGAS was isolated from the superficial skin and biceps femoris as well as the deep soleus and plantaris. The nerve branch innervating the medial GAS was transected to prevent activation of the medial GAS. To attach the LGAS to the muscle lever for force measurements, the Achilles tendon with an attached portion of the calcaneus was cut and tied to the lever arm of a dual-mode servomotor (model 310 B; Aurora Scientific, Aurora, ON, Canada). The muscle was stimulated to contract utilizing a stimulator (Model 2100; A-M Systems, Calsborg, WA) with leads applied to the tibial nerve 1 cm proximal to its insertion into the LGAS. The muscle was kept wet in mineral oil, and the temperature maintained at 36°C with a radiant heat lamp and monitored on the muscle surface with a thermometer. The muscle length was adjusted to the length that produced the highest twitch force, and maximal twitch tension determined. The muscle was stimulated at 150 Hz and 20 V for peak tetanic tension (P_o). Each contraction was followed by 2 min of rest. The servomotor was interfaced with the computer and equipped with an A/D board (National Instruments, Austin, TX). The data were stored and analyzed using LabView software. After the completion of contractile measurements, the muscle was dissected free and weighed.

LGAS in situ *force measurements*

Functional analysis of the DEF ONLY and DEF/REP was identical to the analysis done to the S-D rat muscle samples except that the medial GAS of the Lewis rats was denervated, so that only the LGAS was contributing to force production.

Histology and immunohistochemistry

DEF ONLY and DEF/REP muscles were removed, weighed, and placed in 10% neutral-buffered formalin (Protocol; Fisher Scientific, Waltham, MA) for 24 h, and stored in 70% ethanol until further analysis. Samples were embedded in a Tissue Tech paraffin-embedding system before sectioning on a Reichert-Jung microtome. Within the defect area, at least six, 5 μm sections per muscle were subjected to histologic and immunohistochemical treatment. Hematoxylin and eosin staining was performed, as was Masson's trichrome (Sigma-Aldrich) staining to identify regions of collagen-containing ECM, muscle fibers and other cytoplasmic cells, and nuclei. To observe blood vessels, the rabbit anti-human von Willebrand factor (vWF) polyclonal antibody (1:300; Dako, Carpinteria, CA) was used to identify endothelial cells. The signal was enhanced with biotinylated polyclonal goat-anti-rabbit IgG with streptavidin–horseradish peroxidase. Color was developed after incubation with 3,3-diaminobenzidine. Quantitative analysis of at least six slides at multiple levels throughout the ECM of each rat was performed to determine the number of blood vessels. Muscular infiltration into the ECM was further confirmed by immunofluorescent staining for the muscle-specific cytoskeleton protein, desmin. Sections were exposed to mouse monoclonal anti-desmin antibody (1:500; Sigma-Aldrich). Sections were then incubated with $F(ab')_2$ Goat Anti-Mouse IgG Fluorescein (1:100, $\lambda = 495$ nm; Thermoscientific, Waltham, MA) and counterstained with Hoescht 33258 ($\lambda = 395$ nm; AnaSpec, San Jose, CA) to identify nuclei. Hematoxylin and eosin, trichrome, and vWF sections were observed with a Nikon Diaphot microscope (Melville, NY) mounted with an Optronix Microfire digital camera interfaced with a Dell 8250 computer for storage and analysis of images. Immunofluorescent desmin was observed with a fluorescence microscope (Leica DM LB2, Bannockburn, IL) and photographed with a digital camera (Leica DFC340FX). Quantitative analysis of at least six slides at multiple levels throughout the ECM of each rat was performed with a LabView program to determine the area of each section stained positive for desmin.

Statistical analysis

Means of all measurements were analyzed utilizing Student's *t*-tests for comparison between samples sets or analysis of variance with Tukey's *post hoc* analysis for analysis of groups of samples. Data are represented as mean ± standard error of the mean. Significance is defined as $p < 0.05$.

Results

Immediately upon laceration, the transected myofibers retracted to form a small gap. In LAC, no sign of laceration was apparent macroscopically after 42 days of recovery. No significant difference in isometric tetanic force or muscle weight was apparent between lacerated and control muscles after 42 days of recovery (Table 1).

Immediately upon removal of the muscle defect, theremaining portions of the transected myofibers retracted forming a gap larger than the original defect (Fig. 2A). A gradual remodeling of the LGAS occurred such that at 28 days postdefect injury, little if any of the original defect wound was recognizable (Fig. 2B). Wet muscle weight of the defected LGAS was significantly decreased at all time points relative to the nonoperated contralateral LGAS (Table 2).

Maximal isometric, tetanic tension (P_o) of the whole GAS immediately after the defect injury was 88.3 ± 2.0% and 76.9 ± 3.2% of the contralateral limb for SDEF and LDEF, respectively. After 14 days of recovery P_o was 88.1 ± 5.6% (SDEF) and 80.7 ± 3.5% (LDEF) of the contralateral limb. Twenty-eight days postinjury P_o of LDEF was 79.4 ± 4.0% (Fig. 3, SDEF was not assessed at 28 days). The P_o of the SDEF group was significantly higher than that of the LDEF group at all recovery time points ($p < 0.05$). No significant difference was found at the different recovery time points within each group.

As seen in the S-D rats, immediately upon removal of the defect, the transected myofibers retracted, and if the defect was not repaired, a gradual remodeling took place such that the original defect area was hard to define by 42 days

Table 1. Laceration

LAC 42 days of recovery	
Force (% of control)	103.5 ± 6.3
Control GAS mass (mg)	2883 ± 88
LAC GAS mass (mg)	2950 ± 108

No significant differences between injured and uninjured contralateral control limbs ($p > 0.05$). Values shown are mean ± SEM.

LAC, laceration only; GAS, gastrocnemius; SEM, standard error of the mean.

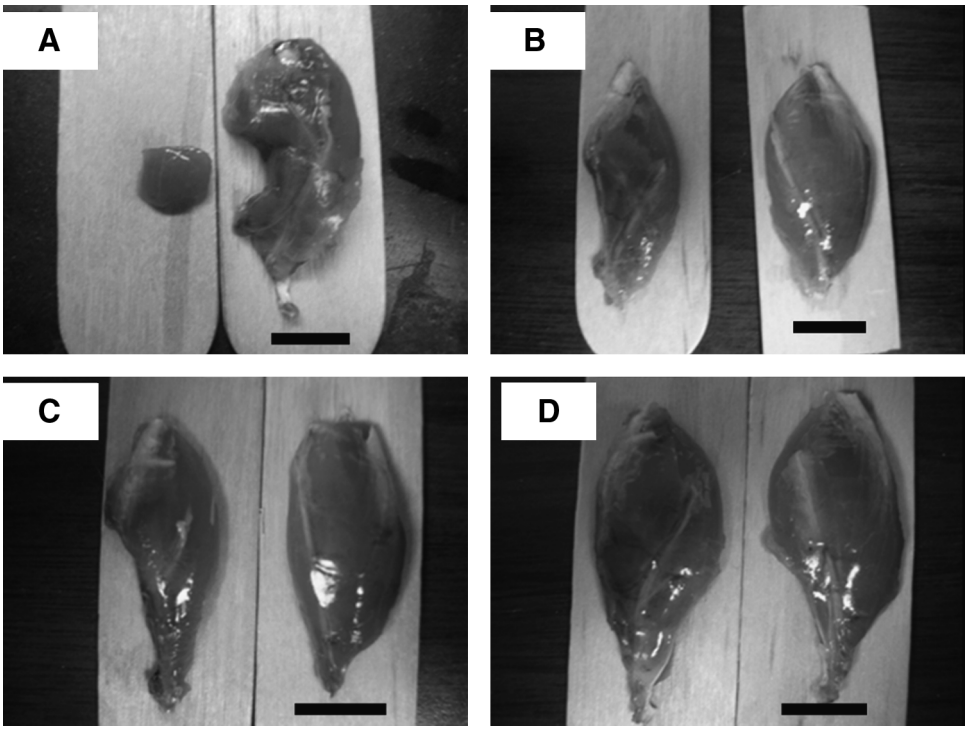

FIG. 2. Defect LGAS morphology relative to contralateral LGAS at (**A**) defect creation, (**B**) 28 days postdefect, and (**C**) 42 days postdefect. (**D**) ECM repair 42 days postdefect (scale bars = 1.0 cm). LGAS, lateral gastrocnemius.

(Fig. 2C). However, repair with the ECM maintained the overall morphology of the LGAS (Fig. 2D).

Before implant, no nuclei or cytoplasm were evident within the decellularized ECMs prior as evidenced by Masson's trichrome staining, and the decellularization protocol removed nearly all soluble proteins as determined by SDS–polyacrylamide gel electrophoresis analysis and Coomassie blue staining (Fig. 1). SDS levels within the ECM before implant were less than 1 μg/mg as determined by colorimetric assay described by Arand *et al.*,[28] which are well below reported cytotoxicity levels for SDS of 10 μg/mg.[30]

Functionally, the maximal isometric, tetanic tension produced by the LGAS of the DEF ONLY group was significantly lower than that of the nonoperated, contralateral limb at all recovery time points. No recovery of force occurred over the course of 42 days in either the DEF ONLY group, nor the ECM repair group (Table 3B and Fig. 4). A statistically significant difference between the DEF ONLY and DEF/REP groups was seen at 7 days postinjury, but not at any subsequent time point. As shown in Tables 3A and 4, the average mass of the defected LGAS with the exception of one was significantly lower than that of the nonoperated, contralateral LGAS. Although the mass of the DEF/REP LGAS tended to be higher relative to the contralateral limb than the mass of the DEF ONLY LGAS, the difference was not statistically significant.

Histological analysis of the defect area with ECM shows the histologic progression of the implanted ECM from 7 to 42 days of recovery (Fig. 5). Immunohistochemistry confirmed the

Table 2. Small Versus Large Defect

	DEF LGAS mass (% of control)		
	0 days	*14 days*	*28 days*
SDEF	92%	82%	—
LDEF	85%	84%	81%

LGAS, lateral gastrocnemius; SDEF, small defect; LDEF, large defect.

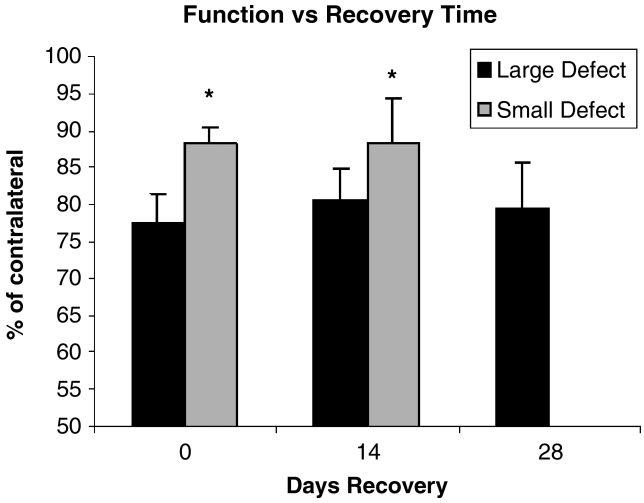

FIG. 3. Sprague-Dawley rat functional data. Gastrocnemius muscles from the large defect group produced significantly less maximal isometric, tetanic tension than those from the small defect group as denoted by asterisks ($p < 0.05$). No data exist for the small defect group at 28 days of recovery.

Table 3A. Mass of Lateral Gastrocnemius in Operated and Non-Operated Limbs

Days of recovery	Defect LGAS wt. (mg)		Contralateral LGAS wt. (mg)	
	DEF ONLY	DEF/REP	DEF ONLY	DEF/REP
7	1054.1 ± 37.3	1400.3 ± 61.6	1271.7 ± 30.4	1257.3 ± 3.7
14	1066.1 ± 29.5	1125.3 ± 43.4	1264.4 ± 20.8	1242.3 ± 18.0
28	1115.5 ± 40.3	1067.8 ± 15.5	1302.8 ± 35.0	1273.4 ± 19.3
42	1054.7 ± 74.1	1102.0 ± 63.3	1283.8 ± 65.9	1261.4 ± 60.7

Values shown are mean ± SEM.

Table 3B. Functional Characteristics of the Lateral Gastrocnemius

Days of recovery	Force (% of contralateral)		Defect force (N)		Control force (N)		Defect SPo (N/cm^2)		Control SPo (N/cm^2)	
	DEF ONLY	DEF/REP	DEF ONLY	DEF/REP	DEF ONLY	DEF/REP	DEF ONLY	DEF/REP	DEF ONLY	DEF/REP
7	68.4 ± 5.1	81.2 ± 8.4	16.3 ± 0.9	18.3 ± 1.5	22.5 ± 0.5	22.5 ± 0.7	16.4 ± 0.5	17.4 ± 1.3	21.0 ± 0.5	24.2 ± 1.2
14	72.9 ± 2.3	77.4 ± 4.2	16.1 ± 0.6	16.1 ± 0.5	22.1 ± 0.5	20.9 ± 0.6	18.6 ± 0.6	18.5 ± 1.0	21.1 ± 0.6	21.7 ± 0.8
28	77 ± 0.8	79.6 ± 3.6	17.2 ± 0.4	16.1 ± 0.7	22.4 ± 0.6	20.3 ± 0.4	19.7 ± 0.4	18.4 ± 0.6	21.5 ± 0.4	20.2 ± 0.6
42	74.1 ± 4.6	77.6 ± 4.8	16.3 ± 1.6	17.3 ± 1.3	21.9 ± 0.8	22.4 ± 1.3	19.5 ± 0.9	19.9 ± 0.7	21.1 ± 0.6	22.9 ± 0.5

Values shown are mean ± SEM.
SPo, specific tension.

presence of desmin-positive myofibers (Fig. 6) and vWF-positive endothelial cells (Fig. 7). Quantification of the desmin-positive area throughout the ECM determined that there were significantly higher numbers of myofibers within the ECM after 42 days of recovery compared to 7 days of recovery, and a significantly higher number of and vWF-positive blood vessels within the ECM at 28 and 42 days compared to 7 days (Table 4 and Fig. 8). Myofibers and blood vessels were found deeper in the ECM as recovery time increased. The area of ECM closest to the border with the transected myofibers appeared most dense with regenerating fibers and blood vessels indicating approximately 1 mm of growth (Fig. 9A). Fewer fibers and blood vessels were seen in the areas deeper into the ECM that were 2–3 mm from the cut muscle surface. Little to no evidence of regenerating fibers or blood vessels was apparent in the middle of the ECM greater than 3–4 mm from the cut muscle surface (Fig. 9B).

Discussion

Little to no regeneration occurs in skeletal muscle after a transection of the myofibers when a substantial amount of the tissue is lost. Regrowth across the muscle defect gap does not occur over the course of 42 days after injury. The remodeling process that takes place during this time makes it unlikely that the muscle would ever return to its original size and shape. Since the maximal isometric, tetanic force immediately postdefect injury is the same regardless of the recovery time allowed, it is likely that permanent functional damage was incurred. Without any significant functional recovery of the muscle and the morphological changes it undergoes, this muscle defect model is a suitable model for use in further investigations into skeletal muscle's regenerative capacity. Since the laceration-only injury showed no functional deficit after 42 days, and the defect injury had not recovered function after 42 days, the defect model presented here could be a better model for the study of skeletal muscle regeneration, and surgical and tissue engineering interventions aimed at regenerating significant amounts of skeletal muscle than a laceration injury model.

Researchers have used GAS laceration models that resulted in a more severe loss of function that, if left unrepaired, persisted for weeks.[31–33] Others, however, have seen functional recovery after only 25 days even in full transection laceration

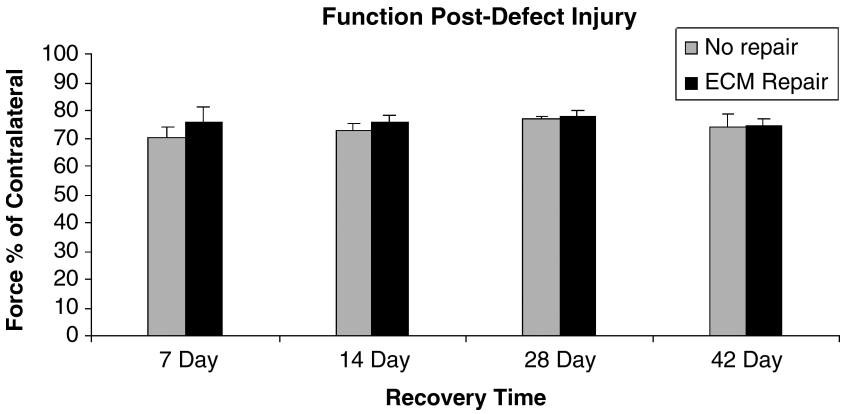

FIG. 4. Maximal isometric, tetanic tension of defect LGAS relative to contralateral limb at 7, 14, 28, and 42 days postinjury. No significant difference between groups or time points.

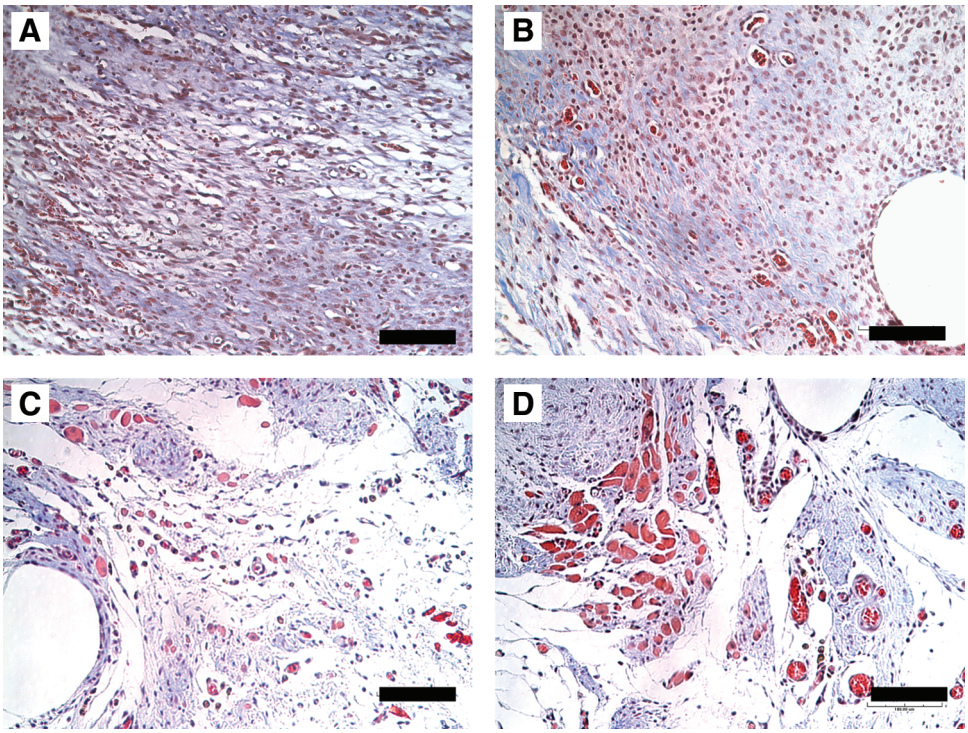

FIG. 5. Masson's trichrome of ECM implant at (**A**) 7, (**B**) 14, (**C**) 28, and (**D**) 42 days of recovery. Note: Circular spaces are suture holes (scale bars = 100 μm). Color images available online at www.liebertonline.com/ten.

models of the soleus.[34] The lack of an apparent functional deficit in this LGAS model after 42 days is likely due to the size and location of the laceration. The laceration was created only on the LGAS and did not transect the medial GAS, but for the laceration model, the mass and force measurements were performed on the whole GAS (medial and lateral together). Additionally, nerve and major blood vessels in the area were left intact, which when taken together with the measurements on the whole GAS likely explains the full functional recovery that occurs in this model, but does not occur in other models where a complete transection of the muscle is performed.[32,33] Further investigation is needed to determine if the LGAS has fully recovered function or if the medial GAS is compensating. However, in the context of our work, we were only attempting to create a laceration as a control injury that was at the same site and to the same depth as the muscle defect. Regardless, the lack of a functional deficit 42 days post-laceration injury underscores the importance of a defect model that demonstrates a functional deficit and has no functional improvement over the same timeframe.

During development of the muscle defect model, two defect sizes were utilized to determine the critical size for

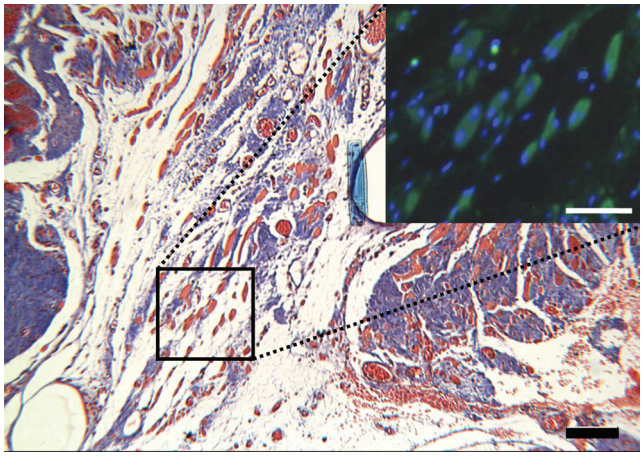

FIG. 6. Masson's trichrome of ECM implant at 42 days of recovery (scale bar = 100 μm) with desmin & Hoescht immunofluorescent–stained inset (scale bar = 50 μm). Color images available online at www.liebertonline.com/ten.

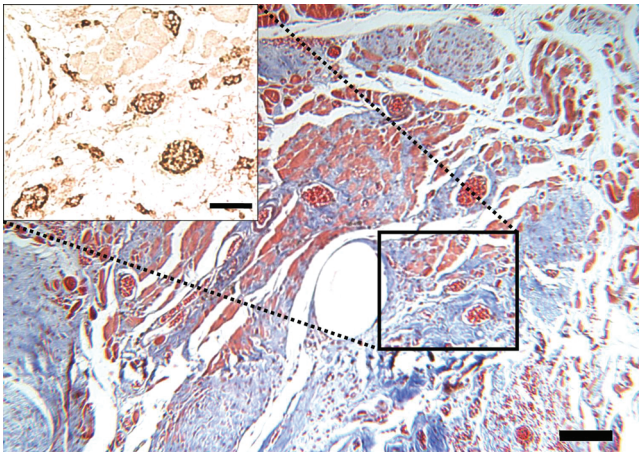

FIG. 7. Trichrome of ECM implant at 42 days of recovery (scale bar = 100 μm) with von Willebrand factor–stained inset identifying presence of blood vessels (scale bar = 50 μm). Color images available online at www.liebertonline.com/ten.

Table 4. Quantification of Desmin-Stained Area and von Willebrand Factor–Stained Blood Vessels Within the Extracellular Matrix Implant

Days of recovery	*Desmin-positive area (% of total)*	*Blood vessels* (n/mm^2)
7	3.9 ± 1.4	7.3 ± 2.9
14	6.4 ± 1.2	11.9 ± 2.7
28	8.0 ± 1.0	14.5 ± 2.4
42	8.2 ± 1.1	14.0 ± 1.8

Significant increase in the desmin-positive area after 28 and 42 days of recovery and in the number of blood vessels at 14, 28, and 42 days of recovery when compared to 7 days ($p < 0.05$). Values shown are mean ± SEM.

establishing significance of our treatment techniques. The 0.5×1.0 cm (~150 mg) defect was not large enough to allow for easy determination of the effectiveness of surgical repair. Although there was a decrease in function that did not begin to return to normal by 14 days (28 days of recovery was not assessed), it was not a large enough functional deficit to allow for definitive evaluation of different repair techniques. The decrease in mass in the SDEF from 92% of contralateral weight to 82% of contralateral weight at day 14 might be explained by the potential for atrophy of the remaining transected myofibers in SDEF. A larger portion of the transected fibers remained in the SDEF and could subsequently experience more atrophy, whereas more mass was initially removed in the LDEF, so smaller portions of transected fibers remained and less mass could be lost due to atrophy. The superior and inferior portions of the LGAS (above and below the defect) were not assessed though. The 1.0×1.0 cm (~306 mg) defect was the maximum size allowed by the rat's anatomy without cutting nerve or major blood vessels supplying distal portions of the limb. Since no functional recovery occurred over 28 days, it was determined that this was a suitable model to study the ability of muscle to regenerate and to evaluate subsequent repair techniques. After the development of the defect injury model in the S-D rats, further experiments were performed on the Lewis rat, an inbred strain of rat better suited for surgical implantation research. Defect surgeries were performed to confirm the lack of functional recovery seen in the S-D rats. Due to minor anatomical differences of the Lewis rat, the 300+ mg defect removed from the S-D rats could not be achieved, and the Lewis rat defect mass was approximately 230 mg. To better isolate the functional effect of the defect on the LGAS, the medial GAS was denervated immediately before force analysis, so that only the LGAS was contributing to force production.

To repair the muscle defect, an implantable material was needed that could bridge the gap between the transected ends of the myofibers and allow mechanical transduction of force. The material also needed to be capable of supporting the growth of myofibers and other muscle-associated cell types. Skeletal muscle ECM was chosen for this reason. The process of decellularizing skeletal muscle to obtain an ECM is possible. The decellularization process removes all cellular components from the tissue so that only the ECM scaffold is left. Acellular tissue is advantageous because the implanted ECM scaffold has physical properties similar to those seen by cells *in vivo*, and the ECM should naturally direct cells to orient in the proper direction. This is important for cells such as muscle progenitor cells activated in the repair process, because they develop best on substances that are most like muscle tissue.[17] Proper alignment of the scaffolding is also important for the transmission of force. A properly derived ECM scaffold is also nonimmunogenic. When implanted, the tissue did not elicit an immune response that would other-

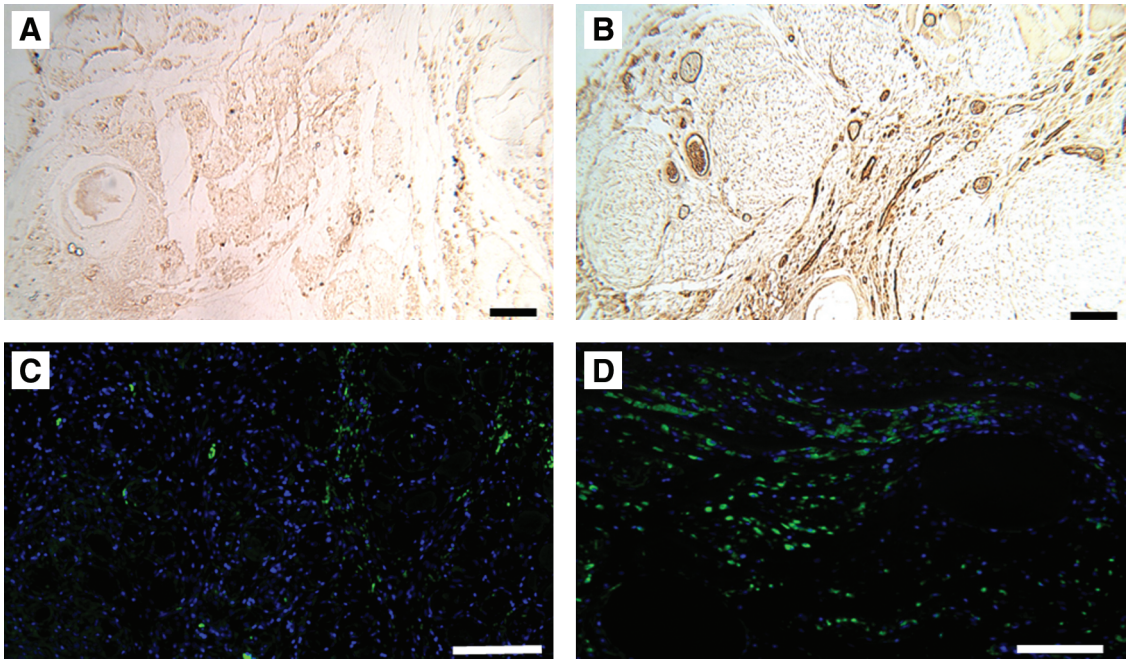

FIG. 8. ECM implant after 7 days stained for von Willebrand factor and desmin (**A, C**) and after 28 days (**B, D**). Scale bar = 100 microns. Color images available online at www.liebertonline.com/ten.

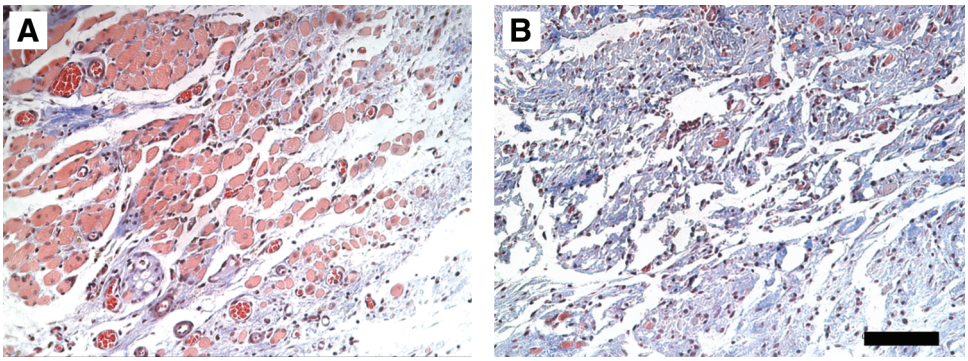

FIG. 9. Serial sections of ECM implant at 28 days of recovery stained with Masson's trichrome. (**A**) 1–2 mm from muscle/ECM border and (**B**) 2–3 mm from muscle/ECM border (scale bar = 100 μm). Color images available online at www.liebertonline.com/ten.

wise reject the implant and render it ineffective, because its immune reactive antigens were stripped off with the cells.[27]

Borschel *et al.* have had success growing viable muscle tissue *in vitro* on an ECM derived from decellularized skeletal muscle.[27] Implantation of acellularized skeletal muscle into muscle defects of the abdominal wall has been performed by several groups with varying levels of success. Although the functional outcome was not assessed, evidence that the ECM is infiltrated by blood vessels is apparent and some researchers have seen infiltration of skeletal muscle fibers as well.[35] Similar results occurred in the implantation of an acellular collagen sponge into defected rabbit vastus lateralis muscles.[36] More successful repair with ECM occurs when myoblasts or satellite cells are seeded onto the ECM before implantation.[24,25,37] Acellular ECM has been successfully employed as a patch to repair defects in a number of tissues, including tendons and cardiac muscle. On their own, ECM scaffolds are effective at repairing tendon injuries of the rotator cuff and Achilles tendon.[38,39] The ECM scaffold bridges the gaps in the tendon and allows incorporation of cells from the native tissue. Similar results have been observed in cardiac muscle with ECM repair. A myocardial ventricular wall defect patched with ECM incorporated more myocardial tissue into the defected area than a synthetic expanded polytetrafluoroethylene (ePTFE) patch used clinically.[40] Defects of the ventricular wall repaired with ECM also lead to increased functional improvements compared to Dacron.[41]

As evidenced by this study, the muscle-derived ECM used here to repair defected skeletal muscle tissue is capable of supporting the growth of blood vessels and myofibers, and is a promising model for the study of muscle regeneration.[27] As recovery time increased, an increase in the number of blood vessels and myofibers was apparent in the ECM at progressively deeper levels, suggesting that the fibers and vessels are growing into the ECM from the transected ends of the surviving myofibers. After 42 days, however, the middle of the ECM was not yet populated with myofibers or blood vessels. The ingrowth of blood vessels seen in the ECMs used in this study has been seen in studies performed on the repair of abdominal wall musculature with similarly derived ECMs.[26,35] Limited ingrowth of myofibers has been confirmed in some of the abdominal wall defect ECM implants,[35] but not all.[24,26,37] The myofiber ingrowth observed in the present study might be due to the difference of the muscles chosen. Functionally, the LGAS is very active and is subjected to a relatively high amount of mechanical stress during normal activity, whereas the abdominal wall musculature does not see the same demands. An increase in the activity level of an injured muscle can expedite the healing process.[42] With the exception of the 7-day recovery time point, the function of the matrix-repaired muscle was not significantly different from the unrepaired muscle up to 42 days postinjury, although longer recovery times were not studied. The reason for the functional improvement of the matrix-repaired muscle compared to the unrepaired muscle after only 7 days of recovery but not at subsequent recovery times is not immediately apparent. The difference could be due to changes in the transected myofibers on the LGAS superior and inferior to the implanted ECM, but these regions of the LGAS were not analyzed. The lack of subsequent functional recovery could be due to the small size and limited number of fibers growing into the ECM, insufficient vasculogenesis throughout the ECM, and possibly incomplete nerve reinnervation of fibers.

In conclusion, the LGAS defect injury model allows for a uniform standard for the study of the regeneration potential after traumatic skeletal muscle injury. This model has tremendous potential to aid researchers in the best treatments to restore function and esthetics to severely damaged skeletal muscle. The muscle defect area could easily be replaced with any of a number of natural or engineered replacement tissues, and regeneration and function could be monitored in the *in vivo* environment as was done with the ECM in this study. The morphology of the repaired LGAS and esthetic appearance were well maintained over 42 days despite the fact that functional recovery did not occur. The possibility exists that longer recovery times greater than 42 days would have given time for better regeneration; however, the ECM provided a suitable environment for blood vessel and myofiber in-growth, which indicates that ECM is a suitable implant material. Further research should focus on increasing the number and size of myofibers throughout the ECM and improving the functional outcome.

Acknowledgment

This work was funded by the U.S. Army MRMC Grant DAMD W81XWH-06-1-0540.

Disclosure Statement

No competing financial interests exist.

References

1. Charge, S.B., and Rudnicki, M.A. Cellular and molecular regulation of muscle regeneration. Physiol Rev **84,** 209, 2004.
2. Jarvinen, T.A., Jarvinen, T.L., Kaariainen, M., Kalimo, H., and Jarvinen, M. Muscle injuries: biology and treatment. Am J Sports Med **33,** 745, 2005.
3. Roth, D., and Oron, U. Repair mechanisms involved in muscle regeneration following partial excision of the rat gastrocnemius muscle. Exp Cell Biol **53,** 107, 1985.
4. LaBarge, M.A., and Blau, H.M. Biological progression from adult bone marrow to mononucleate muscle stem cell to multinucleate muscle fiber in response to injury. Cell **111,** 589, 2002.
5. Palermo, A.T., Labarge, M.A., Doyonnas, R., Pomerantz, J., and Blau, H.M. Bone marrow contribution to skeletal muscle: a physiological response to stress. Dev Biol **279,** 336, 2005.
6. Bartlett, C.S., Helfet, D.L., Hausman, M.R., and Strauss, E. Ballistics and gunshot wounds: effects on musculoskeletal tissues. J Am Acad Orthop Surg **8,** 21, 2000.
7. Owens, B.D., Kragh, J.F., Jr., Macaitis, J., Svoboda, S.J., and Wenke, J.C. Characterization of extremity wounds in Operation Iraqi Freedom and Operation Enduring Freedom. J Orthop Trauma **21,** 254, 2007.
8. Mabry, R.L., Holcomb, J.B., Baker, A.M., Cloonan, C.C., Uhorchak, J.M., Perkins, D.E., Canfield, A.J., and Hagmann, J.H. United States Army Rangers in Somalia: an analysis of combat casualties on an urban battlefield. J Trauma **49,** 515, 2000.
9. Zouris, J.M., Walker, G.J., Dye, J., and Galarneau, M. Wounding patterns for U.S. Marines and sailors during Operation Iraqi Freedom, major combat phase. Mil Med **171,** 246, 2006.
10. Fan, C., Jiang, P., Fu, L., Cai, P., Sun, L., and Zeng, B. Functional reconstruction of traumatic loss of flexors in forearm with gastrocnemius myocutaneous flap transfer. Microsurgery **28,** 71, 2008.
11. Vekris, M.D., Beris, A.E., Lykissas, M.G., Korompilias, A.V., Vekris, A.D., and Soucacos, P.N. Restoration of elbow function in severe brachial plexus paralysis via muscle transfers. Injury **39 Suppl 3,** S15, 2008.
12. Carlson, B.M., and Gutmann, E. Development of contractile properties of minced muscle regenerates in the rat. Exp Neurol **36,** 239, 1972.
13. Vandenburgh, H.H., Karlisch, P., Shansky, J., and Feldstein, R. Insulin and IGF-I induce pronounced hypertrophy of skeletal myofibers in tissue culture. Am J Physiol **260,** C475, 1991.
14. Jenkins, S.D., Klamer, T.W., Parteka, J.J., and Condon, R.E. A comparison of prosthetic materials used to repair abdominal wall defects. Surgery **94,** 392, 1983.
15. Meddings, R.N., Carachi, R., Gorham, S., and French, D.A. A new bioprosthesis in large abdominal wall defects. J Pediatr Surg **28,** 660, 1993.
16. Osses, N., and Brandan, E. ECM is required for skeletal muscle differentiation independently of muscle regulatory factor expression. Am J Physiol Cell Physiol **282,** C383, 2002.
17. Engler, A.J., Griffin, M.A., Sen, S., Bonnemann, C.G., Sweeney, H.L., and Discher, D.E. Myotubes differentiate optimally on substrates with tissue-like stiffness: pathological implications for soft or stiff microenvironments. J Cell Biol **166,** 877, 2004.
18. Engler, A.J., Sen, S., Sweeney, H.L., and Discher, D.E. Matrix elasticity directs stem cell lineage specification. Cell **126,** 677, 2006.
19. Stern, M.M., Myers, R.L., Hammam, N., Stern, K.A., Eberli, D., Kritchevsky, S.B., Soker, S., and Van Dyke, M. The influence of extracellular matrix derived from skeletal muscle tissue on the proliferation and differentiation of myogenic progenitor cells *ex vivo*. Biomaterials **30,** 2393, 2009.
20. Beattie, A.J., Gilbert, T.W., Guyot, J.P., Yates, A.J., and Badylak, S.F. Chemoattraction of progenitor cells by remodeling extracellular matrix scaffolds. Tissue Eng A **15,** 1119, 2008.
21. Reing, J.E., Zhang, L., Myers-Irvin, J., Cordero, K.E., Freytes, D.O., Heber-Katz, E., Bedelbaeva, K., McIntosh, D., Dewilde, A., Braunhut, S.J., and Badylak, S.F. Degradation products of extracellular matrix affect cell migration and proliferation. Tissue Eng A **15,** 605, 2008.
22. Valentin, J.E., Stewart-Akers, A.M., Gilbert, T.W., and Badylak, S.F. Macrophage participation in the degradation and remodeling of ECM scaffolds. Tissue Eng A **15,** 1687, 2009.
23. Badylak, S.F. The extracellular matrix as a biologic scaffold material. Biomaterials **28,** 3587, 2007.
24. Conconi, M.T., De Coppi, P., Bellini, S., Zara, G., Sabatti, M., Marzaro, M., Zanon, G.F., Gamba, P.G., Parnigotto, P.P., and Nussdorfer, G.G. Homologous muscle acellular matrix seeded with autologous myoblasts as a tissue-engineering approach to abdominal wall-defect repair. Biomaterials **26,** 2567, 2005.
25. De Coppi, P., Bellini, S., Conconi, M.T., Sabatti, M., Simonato, E., Gamba, P.G., Nussdorfer, G.G., and Parnigotto, P.P. Myoblast-acellular skeletal muscle matrix constructs guarantee a long-term repair of experimental full-thickness abdominal wall defects. Tissue Eng **12,** 1929, 2006.
26. Gamba, P.G., Conconi, M.T., Lo Piccolo, R., Zara, G., Spinazzi, R., and Parnigotto, P.P. Experimental abdominal wall defect repaired with acellular matrix. Pediatr Surg Int **18,** 327, 2002.
27. Borschel, G.H., Dennis, R.G., and Kuzon, W.M., Jr. Contractile skeletal muscle tissue-engineered on an acellular scaffold. Plast Reconstr Surg **113,** 595, 2004.
28. Arand, M., Friedberg, T., and Oesch, F. Colorimetric quantitation of trace amounts of sodium lauryl sulfate in the presence of nucleic acids and proteins. Anal Biochem **207,** 73, 1992.
29. Kragh, J.F., Jr., Svoboda, S.J., Wenke, J.C., Ward, J.A., and Walters, T.J. Epimysium and perimysium in suturing in skeletal muscle lacerations. J Trauma **59,** 209, 2005.
30. Gratzer, P.F., Harrison, R.D., and Woods, T. Matrix alteration and not residual sodium dodecyl sulfate cytotoxicity affects the cellular repopulation of a decellularized matrix. Tissue Eng **12,** 2975, 2006.
31. Menetrey, J., Kasemkijwattana, C., Fu, F.H., Moreland, M.S., and Huard, J. Suturing versus immobilization of a muscle laceration. A morphological and functional study in a mouse model. Am J Sports Med **27,** 222, 1999.
32. Garrett, W.E., Jr., Seaber, A.V., Boswick, J., Urbaniak, J.R., and Goldner, J.L. Recovery of skeletal muscle after laceration and repair. J Hand Surg [Am] **9,** 683, 1984.
33. Crow, B.D., Haltom, J.D., Carson, W.L., Greene, W.B., and Cook, J.L. Evaluation of a novel biomaterial for intrasubstance muscle laceration repair. J Orthop Res **25,** 396, 2007.
34. Aarimaa, V., Kaariainen, M., Vaittinen, S., Tanner, J., Jarvinen, T., Best, T., and Kalimo, H. Restoration of myofiber

continuity after transection injury in the rat soleus. Neuromuscul Disord **14,** 421, 2004.
35. Vindigni, V., Mazzoleni, F., Rossini, K., Fabbian, M., Zanin, M.E., Bassetto, F., and Carraro, U. Reconstruction of ablated rat rectus abdominis by muscle regeneration. Plast Reconstr Surg **114,** 1509, 2004.
36. Kin, S., Hagiwara, A., Nakase, Y., Kuriu, Y., Nakashima, S., Yoshikawa, T., Sakakura, C., Otsuji, E., Nakamura, T., and Yamagishi, H. Regeneration of skeletal muscle using *in situ* tissue engineering on an acellular collagen sponge scaffold in a rabbit model. ASAIO J **53,** 506, 2007.
37. Marzaro, M., Conconi, M.T., Perin, L., Giuliani, S., Gamba, P., De Coppi, P., Perrino, G.P., Parnigotto, P.P., and Nussdorfer, G.G. Autologous satellite cell seeding improves *in vivo* biocompatibility of homologous muscle acellular matrix implants. Int J Mol Med **10,** 177, 2002.
38. Adams, J.E., Zobitz, M.E., Reach, J.S., Jr., An, K.N., and Steinmann, S.P. Rotator cuff repair using an acellular dermal matrix graft: an *in vivo* study in a canine model. Arthroscopy **22,** 700, 2006.
39. Zantop, T., Gilbert, T.W., Yoder, M.C., and Badylak, S.F. Extracellular matrix scaffolds are repopulated by bone marrow-derived cells in a mouse model of Achilles tendon reconstruction. J Orthop Res **24,** 1299, 2006.
40. Robinson, K.A., Li, J., Mathison, M., Redkar, A., Cui, J., Chronos, N.A., Matheny, R.G., and Badylak, S.F. Extracellular matrix scaffold for cardiac repair. Circulation **112,** I135, 2005.
41. Kochupura, P.V., Azeloglu, E.U., Kelly, D.J., Doronin, S.V., Badylak, S.F., Krukenkamp, I.B., Cohen, I.S., and Gaudette, G.R. Tissue-engineered myocardial patch derived from extracellular matrix provides regional mechanical function. Circulation **112,** I144, 2005.
42. Hwang, J.H., Ra, Y.J., Lee, K.M., Lee, J.Y., and Ghil, S.H. Therapeutic effect of passive mobilization exercise on improvement of muscle regeneration and prevention of fibrosis after laceration injury of rat. Arch Phys Med Rehabil **87,** 20, 2006.

Address correspondence to:
Roger P. Farrar, Ph.D.
Department of Kinesiology
The University of Texas at Austin
1 University Station D3700
Austin, TX 78712

E-mail: rfarrar@mail.utexas.edu

Received: April 3, 2009
Accepted: November 19, 2009
Online Publication Date: January 26, 2010